

TRANSMISSION LASER BONDING OF GLASS WITH SILICON WAFER

Jong-Seung Park and Ampere A. Tseng

Department of Mechanical and Aerospace Engineering
Arizona State University
Tempe, AZ 85287-6106

ABSTRACT

As a microassembly and an encapsulation technique, wafer bonding offers a unique opportunity to combine different materials. Transmission laser bonding not only can satisfy wafer level bonding requirements, but can also be directly implemented into the existing automatic semiconductor fabrication line. In this paper, a laser-induced wafer bonding technique for micro-electro-mechanical systems (MEMS) packaging applications has been investigated using nanosecond pulsed laser. This technique uses specific characteristics of lasers to bond a transparent substrate on top of an opaque substrate. When a focused laser beam with specific wavelength is passed through a transparent wafer, high-density laser energy is absorbed by the target opaque substrate and melts a thin surface layer, which results in a fusion joint to bond two substrates. Pulsed Nd:YAG laser with visible (532 nm) light and 6.5 ns pulse duration is used to demonstrate glass-to-silicon wafer bonding. Laser parameters including laser fluence and focused beam diameter are experimentally determined. The effects of surface condition and contact pressure for the laser bonding technique are examined. The bonded interface is analyzed by Auger electron spectroscopy (AES) and X-ray photoelectron spectroscopy (XPS) to determine drifting or diffusion of atoms between glass and silicon wafers during the laser bonding process. The laser bond strength is measured by tensile test in order to characterize laser bonding quality.

Keywords: Wafer bonding, Laser, Silicon, Glass, MEMS Packaging

INTRODUCTION

In MEMS fabrication, the back-end process involves microassembly and encapsulation of monolithic wafers or diced chips. This packaging process is responsible for more than 70 % of the overall cost of a MEMS device [Reichl, 2001]. Many

MEMS devices are fabricated by integrating micromechanics and microelectronics on the same chip. Henceforth, there is a need for a unified packaging process at wafer level. Currently, each MEMS device has its own specially designed packaging method. There is no universal process for wafer level MEMS packaging. Furthermore, electronics packaging technology is not directly applicable to fabricate mechanical microstructures. Therefore, a major research focus is on electrical and mechanical bonding techniques, which can simultaneously assemble a large number of parts with micro-scale precision. Wafer bonding offers a unique opportunity to combine different materials wherein a cover substrate can be bonded onto a machined substrate. Some of the prominent applications are Silicon-On-Insulator (SOI) wafers [Mitani, 1992], MEMS sensors and actuators [Cohn, 1998], and biomedical devices. Conventional wafer bonding techniques are classified as anodic bonding, direct wafer bonding (or silicon fusion bonding), and intermediate layer bonding (or eutectic bonding), and were mainly developed for the semiconductor industry. Though they exhibit good bonding properties, they require a high processing temperature and a flat surface, furthermore, conventional methods care little about local selectivity of bonding [Wild, 2001]. Also, existing bonding techniques are performed at the IC stage in which the cover layer and the bond area are required to be accurately aligned. In the event of any misalignment, accurately realigning the cover layer and locating the bonding area is a very costly process.

Transmission laser bonding (TLB) technique breaks through the limitations of conventional wafer bonding methods as well as satisfies the requirements of the standard wafer level packaging process. In comparison with conventional bonding techniques, the laser bonding process does not require vacuum or clean room environment, and can be used to join or bond a variety of metallic and non-metallic (ceramic and polymer) materials. Since the setup of the laser bonding technique can be

consistent with those used in the exiting semiconductor fabrication (CMOS) line, the TLB technique can be relatively easier to be integrated into the current fabrication system for high-volume production.

TRANSMISSION LASER BONDING TECHNIQUE

Lasers have been used in material processing and packaging applications for more than two decades because of its advantages such as material versatility, repeatability, minimal distortion in heat affected zone, no tooling to wear out, non-contact clean processing, and flexibility [Dickinson, 2002]. This multi-use, multi-role, and in situ capability is not offered with any of the other advanced materials processing techniques. Due to material versatility and rapid prototyping capability [Tseng, 2001], the laser-induced wafer bonding technique presents a unique application opportunity.

TLB technique induces a laser of a specific wavelength onto a transparent cover substrate, which is placed on top of a machined opaque target substrate. During the bonding process, the laser is transmitted through the transparent cover substrate onto the opaque substrate with more than 90% transmission efficiency. The transmission factor depends on the medium as well as on the incident laser wavelength. Thermal expansion coefficient of the transparent substrate should match that of the opaque substrate to avoid strain and thermal stress in the joints [Madou, 1997]. The transmitted laser energy is concentrated near the surface of the opaque substrate; this highly focused, high-density energy source melts a small portion of the opaque substrate (Figure 1), resulting in a fusion joint between the two substrates. This joint resembles fusion welding or soldering.

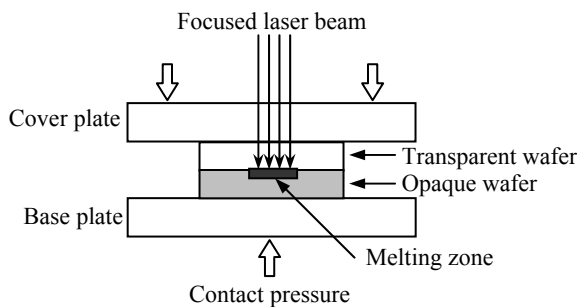


Figure 1. Schematic drawing of laser bonding technique

Laser material interaction has two types: thermal diffusion and ablation. In the thermal diffusion, the heat deposited by the laser diffuses away from the laser interaction zone during the pulse duration. On the other hand, in the ablation, the laser energy is high enough to break atomic bonds to dissolve the target materials. Technically, ablation occurs when the laser pulse duration is shorter than the heat-diffusion time, and laser energy is higher than the bonding energy of the target material. In TLB technique, it is desirable that the laser is operated in the thermal diffusion mode to melt a very small spot of a thin surface layer of the substrate. During bonding, the laser acts as a heat source thereby the surface of the target substrate is heated and ultimately, a phase transition temperature is reached. Then, the target region of the opaque substrate begins to melt.

Wild et al. [2001] and Witte et al. [2002] demonstrated reproducible locally selective silicon-glass (Pyrex type) wafers bonding using continuously emitting Nd:YAG laser with 1064 nm wavelength for 2 ~ 10 seconds irradiation time. Wild et al. used 30 W laser emission powers with 300 μm focused beam diameter to generate 4 \times 4 mm² circle- and square-contour bonds. Using K thermocouples integrated near the beam path (0.3 ~ 1.0 mm), the maximum temperature was measured as 300 $^{\circ}\text{C}$. In dynamic experiments, cracks were generated in glass at the beginning or end of the bonded line due to the high temperature gradient. Tensile test showed 5 ~ 10 MPa bond strength. Witte et al. addressed the narrow parameter window to achieve a circular bond of 3 mm in diameter at 47 W laser power with 300 μm focused diameter. They mentioned that melting of silicon would destroy the single crystal and would result in a poly crystalline structure that would change electrical and mechanical properties of the original structure.

MATERIAL PROPERTIES

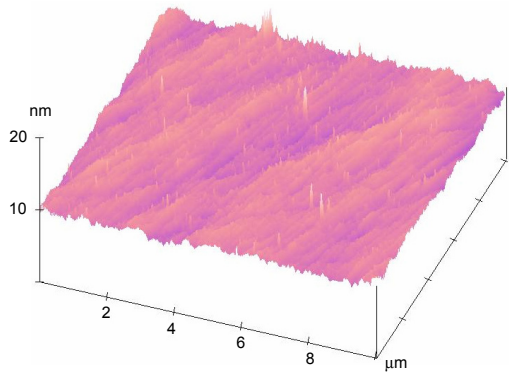
In wafer bonding, the most commonly employed material combination is silicon and glass. Silicon is fabricated into microstructures with excellent mechanical strength and it is possible to integrate electronic circuits in silicon-based microsystems for sensing and actuating purposes. On the other hand, glass is transparent and acts as an insulator, and has good mechanical and chemical properties. Pyrex glass (Corning 7740, Corning Inc.) is broadly used in wafer level anodic bonding and fusion bonding with silicon substrate, because Pyrex and silicon have a near equivalent thermal expansion coefficient ($3.25 \times 10^{-6}/\text{K}$). Silicon-to-glass bonding is requested in the area of optoelectronic components, biomedical devices, and MEMS sensors. In the present experiment, 500 μm thick Pyrex is used as the transmitting substrate, and 500 μm thick silicon as the absorbing substrate.

The surface condition of two contacting substrates is one of the most important parameters in wafer level bonding. A bad surface condition generates many defects in the bonded area and poor bond quality. The basic requirements of the wafer surfaces are sufficient micro-roughness and flatness. Micro-roughness is a local, microscopic surface characteristic of wafer surface irregularities. The surface roughness is commonly characterized by root mean square roughness (R_q), or arithmetic mean roughness (R_a) measured by atomic force microscopy (AFM). The equations for the surface roughness are:

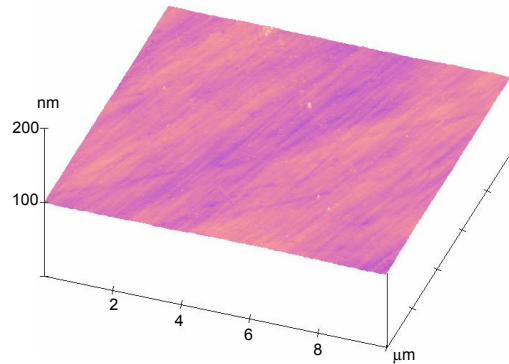
$$R_q = \sqrt{\frac{\sum_{i=1}^n y_i^2}{n}} \quad R_a = \frac{\sum_{i=1}^n |y_i|}{n}$$

where n is the number of data points and y_i is the distance from a datum. Surface flatness is a global, macroscopic surface quality of the wafer surface describing the deviation of the front surface relative to a specified reference plane when the back surface of the wafer is ideally flat, as when pulled down by a vacuum on to an ideally clean flat chuck [ASTM F1530]. In order to specify the flatness of the wafer surface, total thickness variation (TTV) is usually used, which presents the difference between the maximum and minimum values of the thickness wafer [ASTM F533]. Room temperature direct wafer bonding

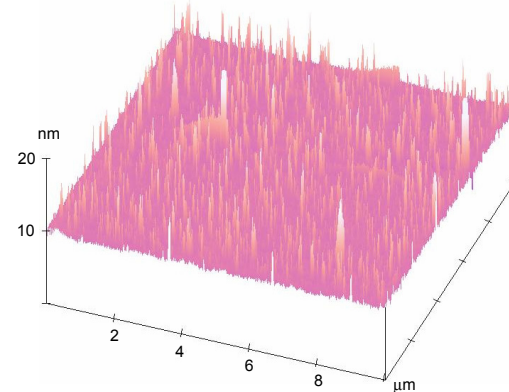
can be succeed with less than 0.5 nm R_q and 1 ~ 3 μm flatness variation over 4-in. silicon wafers [Tong, 1999].



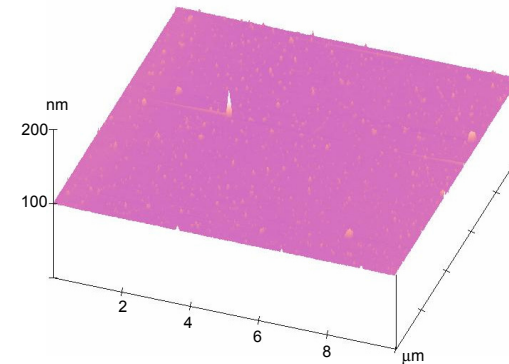
a) Pyrex surface (polished side, 10 nm height scale)



b) Pyrex surface (polished side, 100 nm height scale)



c) Silicon surface (polished side, 10 nm height scale)



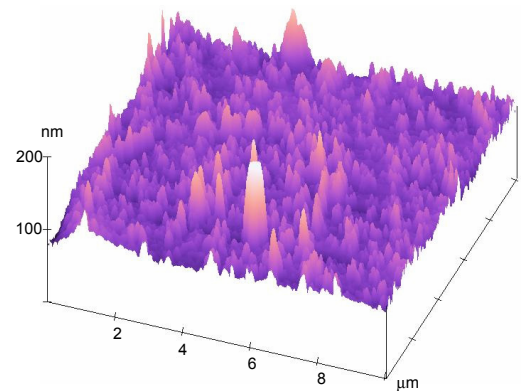
d) Silicon surface (polished side, 100 nm height scale)

Figure 2. AFM image of silicon and Pyrex wafer surface

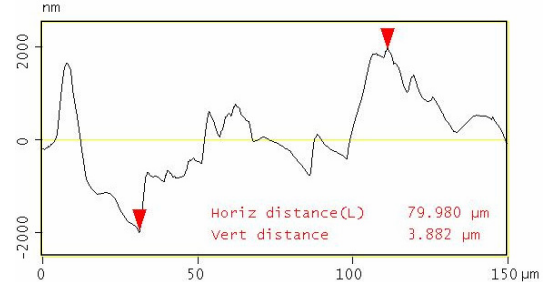
In order to evaluate the surface quality for transmission laser bonding, the surface morphology is measured by AFM (Veeco, Digital Nanoscope III using Si_3N_4 tip (35° tip angle) with 512 line resolution). For surface flatness, TTV is measured over 4-in. silicon wafers and 3-in. Pyrex wafers. The commercial silicon wafers used in the experiment are one-side-polished wafers, and the commercial Pyrex wafers have two-side-polished surfaces. The measured AFM surface images of the polished wafers are shown in Figure 2. The surface morphology is apparently shown with smaller height scale. The results of the measured surface quality are summarized in Table 1. It is found that polished surfaces of silicon and Pyrex wafers have about 0.45 ~ 0.65 nm micro-roughness (R_q), and about 20 μm flatness (TTV). As shown in Figure 3, the unpolished silicon wafer surface has a poor micro-roughness as well as a large deviation in relatively small surface scans.

Parameter	Silicon wafer		Pyrex wafer	
	Polished side	Unpolished side	Polished side 1	Polished side 2
R_q [nm]	0.65	12.74	0.46	0.50
R_a [nm]	0.31	9.22	0.35	0.30
TTV [μm]	14.4		19.5	

Table 1. Surface conditions of silicon and Pyrex wafers



a) AFM image of unpolished silicon surface



b) Surface profile of unpolished silicon surface

Figure 3. Surface quality of unpolished silicon wafer surface

The laser-induced wafer bonding requires that the cover substrate is transparent with respect to the specific laser wavelength and the target substrate opaque to absorb the laser energy. As shown in Figure 4, the transmission of Pyrex glass is approximately 90 % for visible wavelength between 400 nm

and 1000 nm, while silicon has no transmission. Therefore, the laser beam should have a visible wavelength in order to satisfy the requirement of laser bonding.

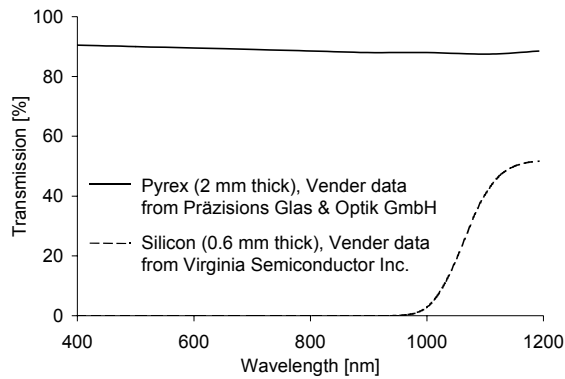


Figure 4. Transmission spectrum of Pyrex and silicon

When silicon or a silicon dioxide surface is exposed to air, a few monolayers of organic contaminants are deposited. These are mainly hydrocarbons and water which, in turn, are rapidly absorbed onto the surface. Interaction occurs between water and other molecules. When other molecules are attracted to water, it is called hydrophilic interaction, and when the ones are repelled water, it is called hydrophobic interaction. For the case of hydrophilic wafers, proper surface treatment is normally accomplished by a standard RCA cleaning prior to the bonding [Bengtsson, 1992]. The attraction force at room temperature between wafer surfaces is caused by hydrogen bonds between hydroxyl (OH) groups and water molecules absorbed on the two wafer surfaces [Tong, 1994]. In this case, the force is electrostatic and relatively weak. For the case of hydrophobic wafers, proper surface treatment is accomplished by dipping it in hydrofluoric (HF) acid prior to deionized water rinsing [Bengtsson, 1992]. In this experiment, wafer-cleaning process is performed by RCA wafer clean procedure to create hydrophilic surface.

EXPERIMENT SETUP

In direct wafer bonding, the contacting process is critical as entrapment of air or particle matter between the surfaces will affect the bond. In order to achieve a good contact between two different substrates, clamping pressure is applied to the substrates to be bonded within a range of 0.1 ~ 2 MPa. A miniature load cell simultaneously measures this during the bonding process. A transparent quartz is used as a cover plate to apply the contact pressure as it allows transmission of the laser beam.

Nanosecond pulsed Nd:YAG laser system is used for wafer bonding. The set-up comprises of Nd:YAG laser, its interface controller, refractive and diffractive optics for beam guidance and focusing, and a precision XYZ stage with a sub-micron positioning resolution, which is controlled by a personal computer. The operating wavelength of Nd: YAG laser is 532 nm (Visible, Green) with 0.2 J pulse energy. With respect to 532 nm visible green laser light, Pyrex wafer is transparent and silicon wafer is opaque. The laser system provides laser pulses with 6.5 ns full width half maximum (FWHM) pulse duration

and a 10 Hz single pulse repetition rate. In Nd: YAG laser bonding system, the incident laser light is focused by a single lens element (Mitutoyo, M Plan NUV 20) of 17 mm focal length as shown in Figure 5. The focal plane position is placed at the interface of the two substrates, transparent and opaque substrates, using the precision XYZ stage and CCD camera. With this setup, the beam diameter is achieved approximately 300 μm at the interface of the two substrates. During the laser bonding process, the clamped Pyrex-silicon wafers are stationary to the incident laser beam. Single laser pulse (6.5 ns duration time) is used to obtain one bond spot to achieve localized bonding. Finally, 8 \times 8 mm² diced silicon-glass wafers are bonded using multiple bond spots.

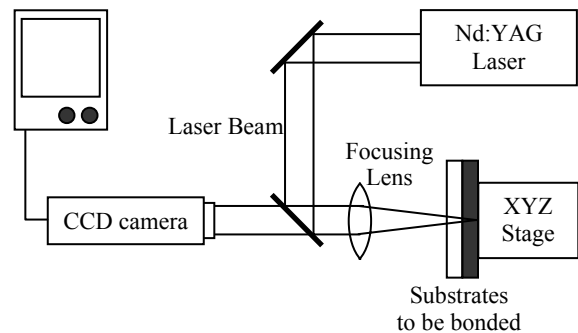


Figure 5. Schematic laser bonding system

The bonded interface is analyzed with Auger electron spectroscopy (AES) and X-ray photoelectron spectroscopy (XPS also referred to as electron spectroscopy for chemical analysis or ESCA) in order to determine drifting or diffusion of atoms at the interface. AES and XPS are the most commonly used techniques for surface analysis with 10 ~ 50 Angstroms below the surface of interest on conducting and semi-conducting solids (Figure 6). Both techniques rely on the emission of secondary electrons from the specimen after the surface has been excited with either electrons (AES with 2 μm spot size) or X-rays (XPS with 2 ~ 3 mm spot size). Samples must be compatible with an ultrahigh vacuum system ($\sim 10^{-9}$ torr. or better). AES allows the incident electron beam to be moved from one specimen surface region to another for determining of the surface elemental distribution. XPS has the sensitivity to detect spectrum peak position energy shifts for determining of chemical bonding states for sample surfaces.

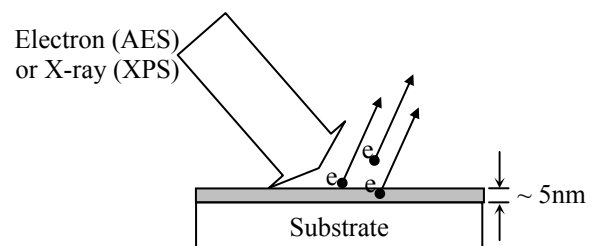


Figure 6. Schematic of Auger electron spectroscopy (AES) and X-ray photoelectron spectroscopy (XPS)

In order to characterize laser bonding quality, a computer controlled micro tensile tester at Integrated Mechanical Testing Laboratory (IMTL), Arizona State University, has been used

(Figure 7). Micro-tester has 150 N maximum uni-axial load with 1 g load and 100 nm displacement resolutions. The bonded sample is glued to the steel fixture using epoxy resin, thereby, the steel fixture is connected to a pull stud. Translation speed of the micro tester is 500 nm/s and sampling rate is 5 points/s. The maximum strength when the substrates begin to peel off is recorded. The bonding strength is calculated by dividing the load needed to separate the bonded sample from the bonded area.

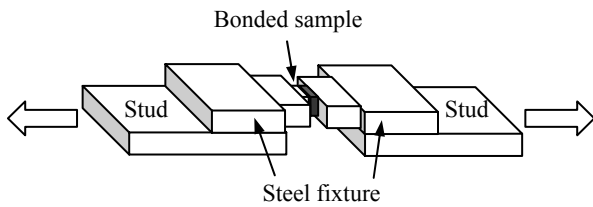


Figure 7. Tensile test setup of laser bond sample

RESULTS AND DISCUSSION

Using a 6.5 nanosecond pulsed Nd:YAG laser bonding system, Pyrex-to-silicon wafers have been successfully bonded between the polished surfaces ($0.45 \sim 0.65 \text{ nm } R_q$) of Pyrex and silicon wafers. Since the unpolished silicon surface has a poor micro-roughness ($12 \text{ nm}, R_q$) and a large surface deviation, laser bonding has not occurred between the polished Pyrex surface and the unpolished silicon surface. A single laser pulse with 200 mJ pulse energy and approximately $300 \mu\text{m}$ diameter focused laser beam size, generates a disc-shaped bond spot with about $250 \mu\text{m}$ spot diameter. With a hundred micron scale bonds, the laser bonding has local selectivity. As shown in Figure 8, $8 \times 8 \text{ mm}^2$ diced Pyrex and silicon wafers are firmly bonded with multiple laser bonded spots separated by $1016 \mu\text{m}$ between bonded spots.

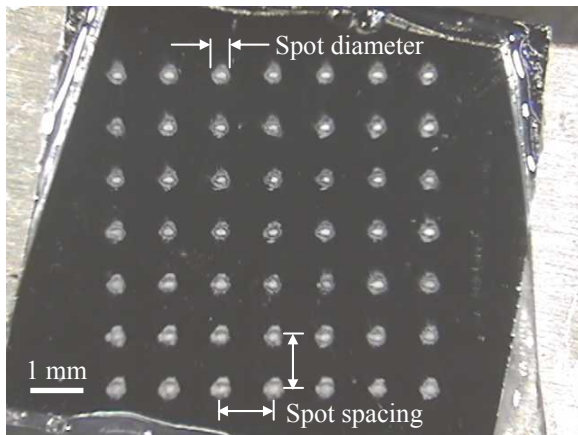
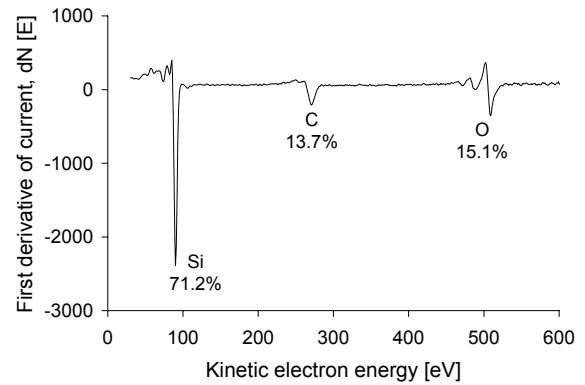


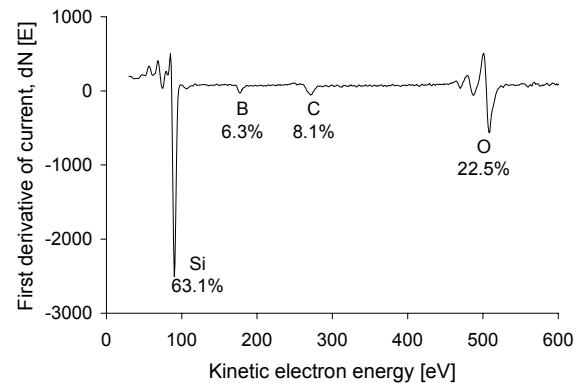
Figure 8. Optical images of localized Pyrex-to-Silicon wafer bonding by pulsed Nd:YAG laser

In order to determine drifting or diffusion of atoms at the bonded interface, the delaminated bonded interface is analyzed with AES (Physical Electronics, SAM 590) and XPS (Kratos, XSAM800). Since AES uses an electron beam (10 keV) to excite the surface, AES cannot analyze insulating solids such as Pyrex glass wafer. However, the small spot size ($2 \mu\text{m}$) of AES

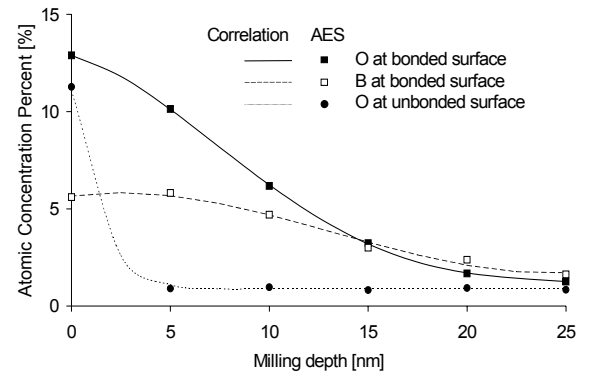
has good spatial resolution to analyze the single laser bonded spot with about $250 \mu\text{m}$ diameter.



a) AES spectrum at the unbonded surface



b) AES spectrum at the bonded interface

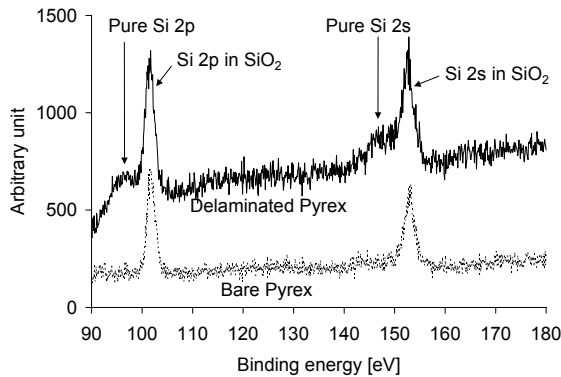


c) The distribution of boron and oxygen at the delaminated silicon surface with to Ar ion milling (4 keV)

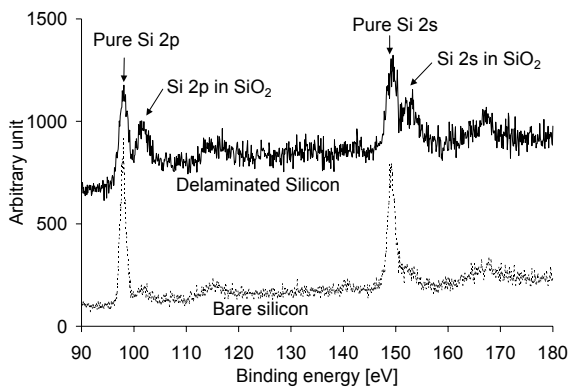
Figure 9. Auger electron spectrum and the distribution profile in depth at the delaminated silicon surface

The Auger electron spectrum and the distribution profiles in depth at the delaminated silicon surface are represented in Figure 9. AES measures that the used silicon wafer surface has a thin native oxide layer and a carbon contamination by air exposure (Figure 9.a). At the bonded surface, boron (B) is detected, and the atomic concentration percentage (22.5 %) of oxygen (O) on the bonded interface is slightly larger than that (15.1 %) on the native oxide layer as shown in Figure 9.b.

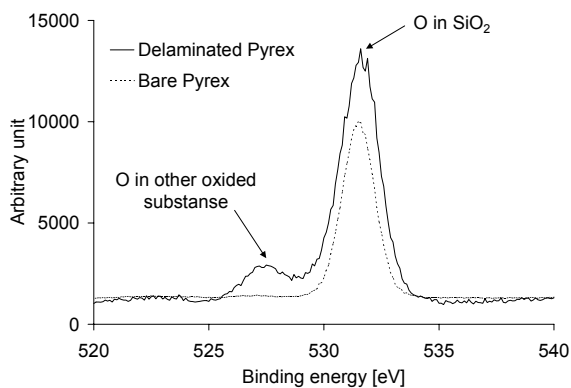
Since Pyrex glass wafer consists of 80 % SiO₂, 10 % B₂O₃, and 5 % Na₂O chemical contents [Bansal, 1986] and the used silicon wafer has no dopants, the boron and the increased oxygen are diffused from Pyrex glass. Figure 9.c shows the depth profiles of the boron and the oxygen with Ar ion (4 keV) milling time with 5 nm/min. of the corresponding milling rate. While the thin native oxide layer is removed by 1 minute milling, the boron and the oxygen at the delaminated surface are distributed in relatively deep silicon substrate. It can be concluded that the temperature at the interface increases to the silicon's melting point by the focused laser energy, which generates the oxygen diffusion.



a) XPS spectrum for silicon on the silicon surface



b) XPS spectrum for silicon element on the Pyrex surface



c) XPS spectrum for oxygen element on the Pyrex surface

Figure 10. X-ray photoelectron spectrum at the bonded interface and the bare silicon & Pyrex surfaces

Since XPS uses X-ray to excite the surface, XPS can analyze conducting and semi-conducting solids as well as insulating solids. Using XPS, both of the delaminated and the bare (after RCA clean) silicon & Pyrex surfaces are analyzed. Since the spot size of XPS is 2 ~ 3 mm, Pyrex and silicon wafers (8 × 8 mm²) are bonded with multiple laser bonded spots with 300 μm spot spacing, which is the focused laser beam size. Figure 10 represents the X-ray photoelectron spectrums at the bare and the delaminated wafer surface. XPS detects spectrum peak position energy shifts for determining of chemical bonding states for sample surfaces. Compared with the bare silicon surface, XPS measures the amount of Si bonded to O (forming SiO₂) increases at the delaminated silicon surface as shown in Figure 10.a. At the delaminated Pyrex surface, the pure silicon is slightly increased, while the bare Pyrex has no pure silicon as shown in Figure 10.b. On the bare Pyrex surface, most of the O belongs to SiO₂. In addition to O belonging to SiO₂, the delaminated Pyrex surface has other O belonging to other oxidized substances, which drifted from inside Pyrex as shown in Figure 10.c. It can be concluded that the temperature gradient at the interface by the focused laser energy generates the drift of the oxidized substances (B₂O₃ or Na₂O) in Pyrex glass to the interface, then the oxygen diffusion toward the melted silicon surface results in covalent Si-O bonds between two wafers.

Tensile test shows that laser bond strength is about 10 MPa as shown in Figure 11. Pyrex and silicon wafers are bonded without any intermediate layer. Anodic bonding at 1 atm. air with 400°C temperature provides 12.4 MPa bond strength [Cozma and Puers, 1995], and fusion bonding does 10 MPa bond strength after 450°C annealing for 5 hours [Xiao et al., 1999]. Therefore, TLB technique has high bond quality as great as the other conventional wafer bonding techniques. In nanosecond pulsed laser bonding, the relation between the contact pressure and the bond strength by tensile test is investigated as shown in Figure 11. It is found that more than 0.5 MPa contact pressure is required to achieve 10 MPa bond strength. The bond strength decreases with less than 0.5 MPa contact pressure. It can be concluded that the tensile strength of TLB has no contact pressure dependence with more than 0.5 MPa contact pressure.

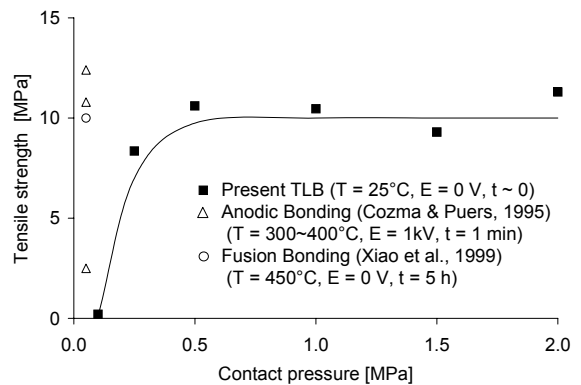


Figure 11. Contact pressure applied in the bonding process versus Pyrex-to-silicon laser bonding strength

CONCLUSIONS

TLB technique at wafer level has been investigated and demonstrated in this paper. Pyrex-silicon wafers have been bonded using nanosecond pulsed Nd:YAG laser of 532 nm (Visible, Green) with 200 mJ energy per pulse. The required wafer surface condition for laser bonding is less than 0.65 nm R_q . Using AES and XPS, it is found that the temperature gradient at the interface generates the drift of the oxidized substances in Pyrex glass to the interface, as the temperature at the interface increases to the silicon's melting point by the focused laser energy. Then, the oxygen diffusion toward the melted silicon surface results in covalent Si-O bonds between the two wafers. Bond strength as per tensile test has been found to be 10 MPa, which is on par with conventional wafer bonding techniques. Critical contact pressure is 0.5 MPa for reliable laser bonding quality, and it has been found that there is no dependence on higher contact pressure. Locally selective laser bonding can be a useful method to assemble miniature devices with very small geometries. In general, TLB technique can not only satisfy wafer level bonding requirements, but can also be directly implemented into the existing semiconductor fabrication line with the implementation issues such as cost-effectiveness, operational simplicity, and extendibility for future requirements [Brannon, 2002]. As a result, this technique is promising high-volume manufacturing of the next generation of microelectronics and microdevice products.

ACKNOWLEDGEMENTS

The authors wish to thank T. Karcher at Center for Solid State Science (CSSS) at Arizona State University for help with AES & XPS measurements and Dr. D. Kingsbury at Integrated Mechanical Testing Laboratory (IMTL) at Arizona State University for help with tensile test.

REFERENCES

1. Reichl, H., Grosser, V., "Overview and Development Trends in the Field of MEMS Packaging", Proc. the IEEE Micro Electro Mechanical Systems (MEMS), 2001, pp. 1-5
2. Mitani, K., Gösele, U.M., "Wafer Bonding Technology for Silicon-On-Insulator Applications: A Review", J. Electronic Materials v 21, n 7, 1992, pp.669-676
3. Cohn, M.B., Bohringer, K.F., Noworolski, J.M., Singh, A., Keller, C.G., Goldberg, K., Howe, R., "Microassembly Technologies for MEMS", Proc. the SPIE-The International Society for Optical Engineering, Santa Clara, California, September 1998, v 3512, pp.2-16
4. Tong, Q.-Y., Gösele, U., "Semiconductor Wafer Bonding: Science and Technology", John Wiley & Sons, 1999, New York
5. Bengtsson, S., "Semiconductor Wafer Bonding A Review of Interfacial Properties and Applications", J. Electronic Materials v 21, n 8, 1992, pp.841-862
6. Wild, M.J., Gillner, A., Poprawe, R., "Locally Selective Bonding of Silicon and Glass with Laser", Sensors and Actuators A 93, 2001, pp.63-69
7. Dickinson, J., "Physical and Chemical Aspects of Laser-Materials Interactions Relevant to Laser Processing (Invited Paper) ", Proc. SPIE-The International Society for Optical Engineering v 4637, San Jose, USA, January 2002, pp.453-464
8. Tseng, A.A. and Vakanas, G.P., "Development of Laser-based Tools for MEMS Rapid Prototyping", Proc. the 2001 NSF Design, Service and Manufacturing Grantees & Research Conference, MPM Paper, National Science Foundation, 2001 (published in CD form)
9. Madou, M., "Fundamentals of Microfabrication", CRC, 1997, New York
10. Witte, R., Herfurth, H., Heinemann, S., "Laser Joining of Glass with Silicon", Proc. SPIE-The International Society for Optical Engineering v 4637, San Jose, USA, January 2002, pp.487-495
11. ASTM F1530, "Standard Test Method for Measuring Flatness, Thickness, and Thickness Variation on Silicon Wafers by Automated Noncontact Scanning", Annual Book of ASTM Standards, v 10.05, 1994, pp.533-539
12. ASTM F533, "Standard Test Method for Thickness and Thickness Variation of Silicon Wafers ", Annual Book of ASTM Standards, v 10.05, 2002, pp.178-182
13. Tong, Q.-Y., Gösele, U., "Semiconductor Wafer Bonding: Recent Developments", Materials Chemistry and Physics, v 37, n 2, 1994, pp.101-127
14. Bansal, N.P., Doremus, R.H., "Handbook of Glass Properties", Academic Press, 1986, New York
15. Cozma, A., Puers, B., "Characterization of the Electrostatic Bonding of Silicon and Pyrex Glass", J. Micromechanics and Microengineering 5, 1995, pp.98-102
16. Xiao, Z.-X., Wu, G.-Y., Li, Z.-H., Zhang, G.-B., Hao, Y.-L., Wang, Y.-Y., "Silicon-Glass Wafer Bonding with Silicon Hydrophilic Bonding Technology", Sensors and Actuators 72, 1999, pp.46-48
17. Brannon, J., "Laser Material Processing: An Industrial View of Packaging Applications", Proc. the SPIE-The International Society for Optical Engineering, San Jose, California, January 2002, v 4637, pp.474-478

Park JS, Tseng AA (2004) Transmission laser bonding of glass with silicon wafer. In: Proceedings of 2004 Japan-USA symposium on flexible automation, paper no. UI-073, American Society of Mechanical EngineersGoogle Scholar. White R, Herfurth H, Heinemann S (2002) Laser joining of glass with silicon. In: Sugioka K et al (ed) Photon processing in microelectronic and photonics. Proceeding of SPIE, vol. 4637. International Society for Optical Engineering, pp487-495Google Scholar. Wiegand M, Reiche M, Gosele U, Gutahr K, Stolze D, Longwitz R, Hiller E (2000) Wafer bonding of silicon wafers covered with various surface layers. Sensor Actuat A A86:91-95CrossRefGoogle Scholar.